Time-to-space mapping of femtosecond pulses

Martin C. Nuss, Melissa Li,* and T. H. Chiu

AT&T Bell Laboratories, 101 Crawfords Corner Road, Holmdel, New Jersey 07733

A. M. Weiner

Department of Electrical Engineering, 1285 Electrical Engineering Building, Purdue University, West Lafayette, Indiana 47907

Afshin Partovi

AT&T Bell Laboratories, 600 Mountain Avenue, Murray Hill, New Jersey 07974

Received December 17, 1993

We report time-to-space mapping of femtosecond light pulses in a temporal holography setup. By reading out a temporal hologram of a short optical pulse with a continuous-wave diode laser, we accurately convert temporal pulse-shape information into a spatial pattern that can be viewed with a camera. We demonstrate real-time acquisition of electric-field autocorrelation and cross correlation of femtosecond pulses with this technique.

During the past few years, various groups have reported shaping of short optical pulses by use of linear filtering in the frequency domain.[1–5] This technique is highly attractive, as it performs operations such as matched filtering and generation of specific pulse patterns in the Fourier (spectral) domain in parallel, rather than serially, in the time domain. Recently this technique has been extended to temporal holographic processing of femtosecond light pulses in the frequency domain,[6,7] and storage and recall of femtosecond pulses as well as some elementary signal-processing operations were demonstrated with this technique.[8] It is striking how closely such a temporal holography setup resembles the Fourier-transform correlator,[9] which is used in optical image correlation and spatial pattern recognition.[10] This resemblance is no accident: while a spatial correlator records a hologram of the spatial frequencies k of the object shape, a temporal correlator records a hologram of the temporal frequencies ω of the pulse shape.

The similarity between spatial and temporal Fourier-transform holography opens up the possibility of mixing temporal and spatial information and may lead to numerous applications ranging from temporal pattern recognition to multiplexing, demultiplexing, and routing of optical signals. In this Letter we demonstrate the fundamental equivalence of time and space in Fourier-transform holography. We show that with this equivalence we can convert temporal information directly into spatial information. The use of a novel multiple-quantum-well (MQW) photorefractive device as a fast holographic medium further allows us to record and read such holograms in real time. As a first demonstration, we apply this technique to measure electric-field autocorrelation and cross correlation of femtosecond pulses in real time.

For formation of a temporal hologram, a signal pulse $E_S(t)$ carrying the temporal information and a short, featureless reference pulse $E_R(t)$ are spectrally dispersed by a diffraction grating in the input plane, collimated by a lens, and interfere in a holographic medium placed at the spectrum plane (Fig. 1). The intensity of the interference fringes in the spectrum plane is described in the Fourier domain as[8]

$$|E_S(\omega) + E_R(\omega)|^2 = |E_S(\omega)|^2 + |E_R(\omega)|^2 + E_S^*(\omega)E_R(\omega) + E_S(\omega)E_R^*(\omega). \quad (1)$$

This equation also describes the fringes recorded in a spatial Fourier-transform correlator when ω is replaced by k. When the fringes are read out with a point source (in time or space), either one of the last two terms in Eq. (1) describing correlations of signal and reference is recovered. The equivalence between spatial and temporal holography becomes even more transparent when we describe the action of the grating in the space–time domain. It is known that the effect of the grating on an optical pulse $E_0(t)$ is found by multiplying its spectrum $E_0(\omega)$ with a complex filter function[11]:

$$E(x, \omega) = \exp[i\beta(\omega - \omega_0)x/c]E_0(\omega), \quad (2)$$

where the x axis points along the surface of the input plane and lies in the plane defined by input and diffracted beams, ω_0 is the center frequency of the pulse, $\beta = \omega_0 \, d\theta/d\omega = \lambda_0/d \cos\theta$ is the dispersion parameter of the grating, $\lambda_0 = 2\pi c/\omega_0$, d is the pitch of the grating, θ is the angle of diffraction, and c is the speed of light. Transforming back into the time domain, we find that immediately behind the grating the diffracted optical pulse has the form

$$E(x, t) = E_0(t - \beta^x/c). \quad (3)$$

This equation describes a spatial image of the input pulse projected onto the grating, with a time-to-space scaling factor of β/c and surfing across the grating

0146-9592/94/090664-03$6.00/0

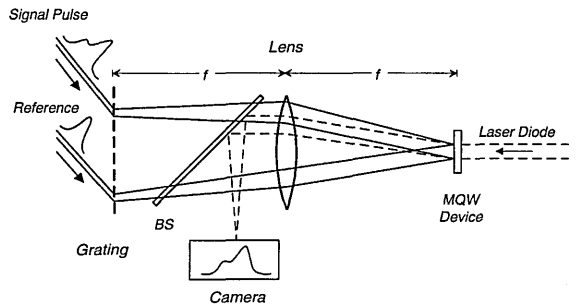

Fig. 1. Schematic of our setup for time-to-space mapping. Although a transmission grating is shown here for clarity, the experiment uses a regular reflection grating.

at a speed $v = c/\beta$. A conversion of the temporal information into spatial information has taken place in the grating plane, and the signal pulse shape is present (in amplitude and phase) as a spatial image in this plane. Hence the temporal holography setup is identical to a spatial correlator,[10] in which scaled versions of the pulse shapes are presented as images by a screen or a spatial light modulator in place of the grating. The only difference between an image from a screen or light modulator and from a temporal pulse is that the image from the pulse is not static but surfs across the grating at a speed c/β. However, as long as the reference pulse does the same, the interference fringes in the spectrum plane S will be stationary and can be recorded as a hologram.

The idea behind the present experiment is that, once the hologram is written, one cannot fundamentally distinguish whether the hologram was recorded with the use of temporal or spatial information. Consequently this offers the opportunity of converting temporal data into spatial data and vice versa. For example, in the experiment described below we accomplish time-to-space mapping by writing a temporal hologram with spectrally dispersed pulses but then interpret the temporal hologram as a spatial hologram by reading it out with a monochromatic plane wave (Fig. 1). Conversely, one can achieve space-to-time mapping by using a spatial light modulator to write a spatial hologram and then reading out the hologram with a spectrally dispersed short optical pulse.

In the experiment, we use a 600-line/mm diffraction grating and a 200-mm focal-length Fourier-transform lens. The center wavelength λ_0 of the femtosecond laser is approximately 830 nm, and each of the two beams has approximately 5-mW average power. The angle of incidence is chosen so that the diffracted beam is parallel to the surface normal of the grating in all our experiments (i.e., $\theta = 0°$, so that $\beta = \lambda/d$). A MQW photorefractive device, located at the spectrum plane, serves as a real-time holographic medium.[2] Since the MQW photorefractive device is not the main subject of this Letter, we refer the reader to previously published reports for details.[2,12] The MQW device has a response time of less than 1 μs at an energy density of 1 μJ/cm^2 and a diffraction efficiency of a few percent. It is read out with a few milliwatts of power from a collimated single-mode diode laser at 850 nm. At this wavelength, just below the exciton peak of the MQW, the diffraction efficiency of the device is the largest.[12] The diffracted light travels back through the setup, is being picked off by a thin beam splitter, BS, and is focused onto the detector plane by a second Fourier-transform lens of 190-mm focal length (for clarity, Fig. 1 shows only a single lens for both these processes). The correlation peaks in the detector plane are recorded either by a CCD video camera or by a silicon diode array. For the experiments given below, we used a 1024-element silicon diode array with a 25-μm pixel-to-pixel spacing.

Figure 2 shows the correlation peaks for different time delays between the signal and reference pulses in the case for which both the signal and the reference are identical 100-fs laser pulses. The time delay between successive traces is 333 fs. As the time delay between the two input pulses is varied, the correlation peaks move on the detector array. We can obtain a calibration of the time-to-space mapping process by plotting the position of the correlation peaks versus the time delay between the two femtosecond input pulses (see the inset of Fig. 2). This calibration constant is 1.684 $\pm$ 0.03 fs/μm. The calculated calibration constant, when we take into account the different writing and reading wavelengths λ_w and λ_r as well as the different focal lengths f_w = 200 mm and f_r = 190 mm, is given by

$$\frac{\Delta t}{\Delta x} = \frac{\beta}{c}\frac{\lambda_w f_w}{\lambda_r f_r}, \tag{4}$$

which gives $\Delta t/\Delta x$ = 1.703 fs/μm, close to the experimentally obtained value. Figure 2 also shows that there is a limited range over which the input delay can be changed and one is still able to see a correlation peak. This window ΔT results from the finite beam size at the grating. All temporal information projected onto the grating plane has to fit within the beam size without truncation. Another yet identical way of looking at this window is that the input pulses are spread out by the grating to a duration ΔT corresponding to the inverse of the spectral resolution $\Delta\nu$ of the setup. Only if the delay between the two pulses is less than ΔT will the pulses be able to interfere in the MQW. In our particular setup with a beam diameter of 3 mm, this window is approximately 7 ps. For a 1200-line/mm grating, ΔT = 45 ps, and for larger beam diameters, the window can be hundreds of picoseconds, assuming that the diffracted beam always leaves the grating in the direction of the surface normal.

The FWHM of the first-order correlation peaks is 85 μm, which translates into 145 fs. Assuming a sech^2-shaped pulse, this is very close to the theoretical electric-field autocorrelation width of a 100 fs pulse. It may be noted in this context that generally the field autocorrelation is the Fourier transform of the spectrum of the pulse. In the particular case of transform-limited pulses, however, the square of the field autocorrelation closely resembles the standard intensity autocorrelation.

When the signal pulse is longer than the input pulse, we obtain the square of the electric-field cross

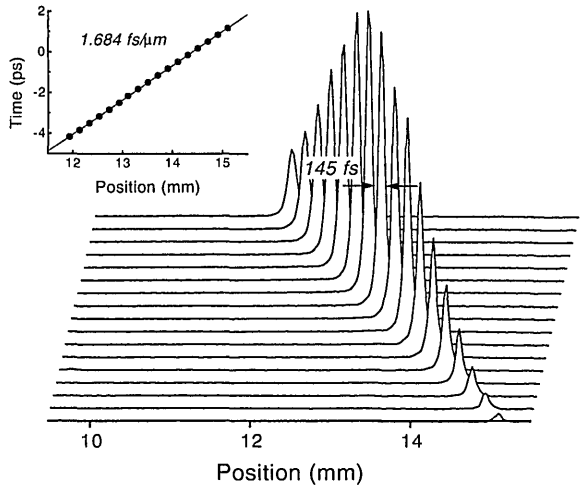

Fig. 2. Autocorrelation peaks as recorded by an array detector in the detector plane with 100-fs pulses for both the signal and the reference beams. The different traces are for different time delays between both pulses, with a 333-fs delay between successive traces. The FWHM of each peak is 85 μm, corresponding to approximately 145 fs. The inset shows the position of the correlation peaks as a function of the time delay between the two input pulses.

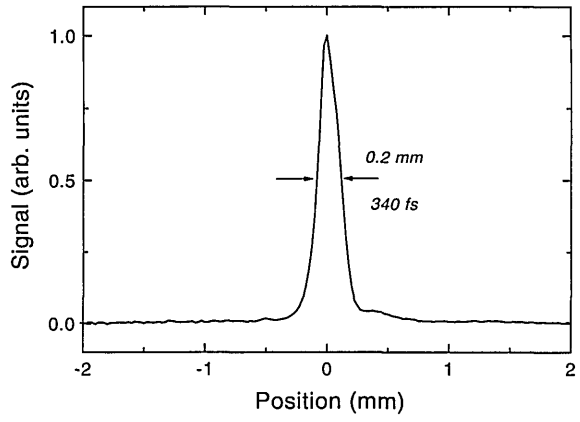

Fig. 3. Cross correlation between two 100-fs pulses, where one of the pulses has been stretched by propagation through a 50-cm-long single-mode fiber. Compared with that in Fig. 2, the FWHM is broadened to 0.2 mm (~340 fs).

correlation between signal and reference pulse. To demonstrate this, we let one of the 100-fs pulses propagate through approximately 50 cm of single-mode fiber to stretch out the pulse duration. The power in the fiber is less than 5 mW, so that mainly linear dispersion occurs in the fiber without much self-phase modulation. Then the signal pulse emerges from the fiber stretched out and with a linear frequency chirp. The cross-correlation profile recorded in the detector is shown in Fig. 3. The FWHM is now 200 μm, corresponding to 340 fs. Within a few percent, the same pulse duration is also measured by conventional intensity cross correlation at the setup. The pulse is also slightly asymmetric, presumably because of some third-order dispersion. It is illuminating to compare the case of chirped and unchirped pulses in the spectral domain by looking at the interference fringes recorded in the MQW. For the two transform-limited pulses, the time delay results in a linear spectral phase shift, which in turn results in equidistant fringes, with the pitch becoming smaller with increasing time delay. As the pitch varies, the diffracted diode laser beam is steered into different directions. For the pulse that has propagated through the fiber, the fiber dispersion leads to a quadratic phase shift, resulting in a chirped hologram with a fringe spacing linearly varying over the width of the hologram. The diffracted beam will be defocused from such a hologram, leading to a larger correlation spot on the detector array.

In conclusion, we have demonstrated conversion of temporal information into spatial information in Fourier-transform holography. The key to the understanding of our experiment is that there is no significant difference between recording a temporal hologram, in which temporal frequencies (wavelengths) are recorded, and recording a spatial hologram, in which spatial frequencies are recorded. The temporal hologram can then equally be read out with a continuous-wave laser, thus permitting the temporal information recorded in the hologram to be interpreted as spatial information. As a first demonstration of this principle, we measure autocorrelation and cross correlation of femtosecond laser pulses with a video camera in real time. We suggest that this technique will open a new field of spatiotemporal holographic processing, in which time and space can be interchanged and converted into each other at will.

*Present address, E. L. Ginzton Laboratory, Stanford University, Stanford, California 94305.

References

1. A. M. Weiner, J. P. Heritage, and E. M. Kirschner, J. Opt. Soc. Am. B **5,** 1563 (1988).
2. M. Haner and W. S. Warren, Appl. Phys. Lett. **52,** 1458 (1988).
3. T. Kobayashi and A. Morimoto, in *Picosecond Electronics and Optoelectronics,* T. C. L. Sollner and D. M. Bloom, eds., Vol. 4 of OSA Proceedings Series (Optical Society of America, Washington, D.C., 1989), p. 81.
4. K. Ema and F. Shimizu, Jpn. J. Appl. Phys. **29,** 631 (1990).
5. A. M. Weiner, D. E. Leaird, J. S. Patel, and J. R. Wullert II, IEEE J. Quantum Electron. **28,** 908 (1992).
6. A. M. Weiner, D. E. Leaird, D. H. Reitze, and E. G. Paek, Opt. Lett. **17,** 224 (1992).
7. Y. T. Mazurenko, Appl. Phys. B **50,** 101 (1990).
8. A. M. Weiner, D. E. Leaird, D. H. Reitze, and E. G. Paek, IEEE J. Quantum Electron. **28,** 2251 (1992).
9. C. S. Weaver and J. W. Goodman, Appl. Opt. **5,** 1248 (1966).
10. A. Partovi, A. M. Glass, T. H. Chiu, and D. T. H. Liu, Opt. Lett. **18,** 906 (1993).
11. O. E. Martinez, Opt. Commun. **59,** 229 (1986).
12. A. Partovi, A. M. Glass, D. H. Olson, G. J. Zydzik, H. M. O'Bryan, T. H. Chiu, and W. H. Knox, Appl. Phys. Lett. **62,** 464 (1993).